Research Article

Simulation of a highly birefringent photonic crystal fiber in terahertz frequency region

Md. Ekhlasur Rahaman[1] · Himadri Shekhar Mondal[1] · Md. Bellal Hossain[1] · Md. Mahbub Hossain[1] · Md. Shamim Ahsan[1] · Rekha Saha[1]

Received: 11 January 2020 / Accepted: 15 July 2020 / Published online: 28 July 2020

Abstract
We have designed a Photonic Crystal Fiber (PCF) to achieve high birefringence optical property in the terahertz (THz) frequency region. Air holes look like rectangular shape in cladding area and elliptical air hole in the center zone are considered for the proposed PCF. To identify loss characteristics of the proposed PCF, effective material loss (EML) and confinement loss also have been studied in this paper. The commercial optical properties analyzer, COMSOL Multiphysics 5.3a software has been used for numerical analysis of the designed PCF. To obtain the optimal PCF structure properties, we have varied the elliptical shaped air holes major axis length and adjacent ellipse pitch distance. Numerical analysis shows the maximum birefringence of 0.0921 and minimum confinement loss of 1.36 $\times 10^{-4}$ cm^{-1} for the proposed PCF. We hope that this highly birefringent PCF will contribute in the field of polarization filter, bio-sensing and terahertz communication devices.

Keywords Birefringence · Confinement loss · Polarization analyzer · PCF

1 Introduction

Photonic crystal fiber (PCF) includes a variety of orientations and tiny air pores that extend through the whole fiber [1]. Due to the extensive benefits of PCF over conventional optical fiber, the use of PCFs in the field of communications, sensing, waveguide, polarization filter is increasing day by day. Research on PCF designing also improving by considering various important optical properties like birefringence, dispersion, confinement loss and effective materials loss etc.

Recently, the PCF sensor that can work on terahertz frequency region and other wavelengths has been able to attract many researchers to design PCF based liquid sensor, gas sensor, temperature sensor [2–8]. Maintaining the polarization effects of those sensors are also important as well as high sensitivity. Polarization effects of an optical system can be reduced by introducing highly birefringent fiber [9]. The birefringence properties of an optical device is defined as the maximum difference between *x* and *y* polarization refractive indices exhibited by the material [10].

There are several research on designing and performance analysis of birefringent PCF with considerable confinement loss in terahertz frequency region. But, before terahertz wave-guide research, in mid-infrared frequency region there are also some study to analysis the birefringence of PCF. Saha et al. [11] designed two different PCF structures for analyzing the elliptical air hole effects on birefringence on their study and they have obtained maximum birefringence of 0.0275 at 1.55 µm wavelength. A circular shaped core area has been studied in [12] where the obtained birefringence is about 0.03. To get higher birefringence, Hasan et al. [13]

✉ Md. Ekhlasur Rahaman, ekhlaseceku@gmail.com | [1]Electronics and Communication Engineering Discipline, Khulna University, Khulna, Bangladesh.

proposed a spiral structure based PCF to maintain the polarization in the wave guide propagation with birefringence value of 0.048 at 1 THz operating frequency but a noticeable EML of 0.08 cm^{-1} is also found. Again, Habib et al. [14] proposed a single mode PCF to improve the birefringence value of 0.051 with slightly lower material loss presented in [13]. But, there is still scope to improve the birefringence and reduce the material loss, confinement loss with fabrication friendly PCF proposal.

In this study, a rectangular shaped PCF has been proposed to achieve high birefringence along with low EML and confinement loss. The core area is considered with three elliptical shaped air holes with same major axis but different length of minor axis. The asymmetrical structure in core and cladding region helps us to achieve an ultra high birefringence in the THz operating frequency region. Topas optical glass has been used in our designed PCF as cladding material. We strongly believe that the considerable width and height of the rectangular air hole will make the fabrication process more flexible. The manuscript is organized as follows: Sect. 2 outlines the design methodology where geometrical structure of the proposed PCF will be discussed. Section 3 addresses the result and discussion and, finally, this will be followed by a conclusion section.

2 Design methodology

Figure 1a shows the cross section vision of the suggested PCF for THz applications. The total dimension of the proposed PCF without PML layer is 2040 µm and the thickness of PML layer is 122 µm. The proposed PCF has two vertically oriented rectangular shaped air holes and six horizontally oriented rectangular shaped air holes in the cladding region with a strut distance of 10 µm. In the core area there are three horizontally oriented elliptical shaped air holes. The height and width for both vertical air holes are denoted by H1 and W1 respectively. Air holes on the upper part and lower part of the core has a same height and width which is denoted as H2 and W2 respectively. Air holes inserted in the left side and right side of the core area also have same height and width which is denoted as H3 and W3 respectively. Free triangles are used to mesh the computational domain where sequence type was physics-controlled mesh. The proposed PCF has 12,592

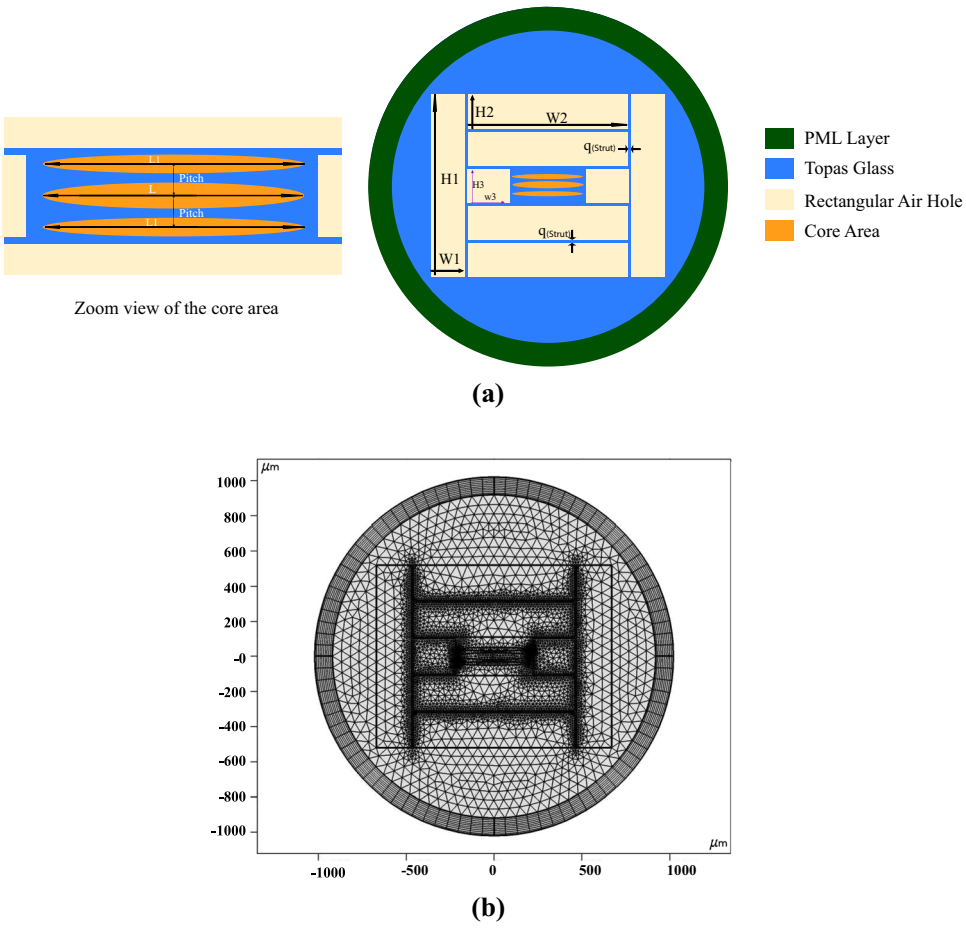

Fig. 1 **a** The cross section view of the proposed PCF. where, H1 = 1040 µm, W1 = 200 µm, H2 = 200 µm, W2 = 920 µm, H3 = 200 µm, W3 = 240 µm, **b** The mesh details of the proposed PCF

domain elements and 1385 boundary elements. Number of degrees of freedom solved for using the software was 94,243. In this study, we have considered the TM mode for calculating all the optical parameters.

During simulation and numerical analysis of the proposed PCF, the height and width of cladding air holes are kept constant. On the other hand, major axis length of the elliptical air holes is varied to find out the optimal condition with maximum birefringence by keeping the minor axis as constant. The major axis length of the center ellipse is denoted by *L*. The major axis length of Upper ellipse and lower ellipse is denoted by *L1*. Center to center distance of adjacent ellipse is called pitch. To find optimal structural conditions of the proposed PCF, the pitch among the adjacent ellipse and strut distance among the rectangular air holes are also varied along with the major axis length.

There are several optical glasses for designing PCF but we have decided to use Topas glass as a background material because of its 0.2 cm^{-1} material absorption coefficient. The Topas glass also exhibits a steady RI of 1.53 from 0.1 to 1.5 THz [15, 16]. For this reasons we have choose the operating frequency of our proposed PCF from 0.5 to 1.5 THz so that by changing the frequency hasn't any effect on the refractive index of Topas glass. The numerical analysis of the proposed PCF carried out by COMSOL Multiphysics 5.3a software with a perfectly matched layer (PML) that absorbs boundary conditions during the simulation process. The effective mode indices were determined by using FEM to resolve a proper value resulting from the Maxwell equation [17]. The PML boundary layer like an anti-reflective surface which absorbs the PCF's outgoing waves [18].

3 Results and discussions

Figure 2a–f shows the light absorption of the fundamental mode in *x* and *y* directed light propagation for the proposed PCF. Figure 2a, b show *x*-polarized effective mode and *y*-polarized effective mode when the major axis length of center ellipse is greater than upper and lower ellipse major axis length. Figure 2c, d show *x*-polarized effective mode and *y*-polarized effective mode when the major axis length of the center ellipse is equal to the upper and lower ellipse major axis length. Figure 2e, f show *x*-polarized effective mode and *y*-polarized effective mode when the major axis length of center ellipse is less than the upper and lower ellipse major axis length.

Depending on these three phenomena, we have calculated the birefringence of the proposed PCF and find out the optimal conditions for which the birefringence is maximum. There is a great impact on electric field distributions due to *x*-polarized and *y*-polarized mode for different lengths of ellipse. For these reasons, there is a large margin difference between effective mode indices of *x*-polarized and *y*-polarized mode which led to get high birefringence. The obtain effective mode index from COMSOL simulator is presented in Fig. 3 along with frequency change for different length combinations of ellipse as mentioned previously. The solid line represents the *x*-polarized effective mode index and dash line represents the *y*-polarized effective mode index. Birefringence is a positive subtracted value of *x* and *y* polarization effective mode index and its mathematical expression is showing in the following equation [19]

$$\text{Birefringence } (B) = |r_x - r_y| \tag{1}$$

where r_x denotes real part of *x*-polarized effective mode index and *y*-polarized effective mode index the real part is r_y.

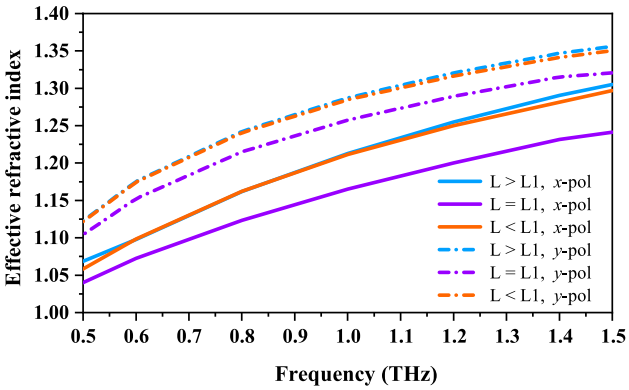

Fig. 3 Effective mode index of the proposed PCF along with frequency change for *x* and *y* polarization mode

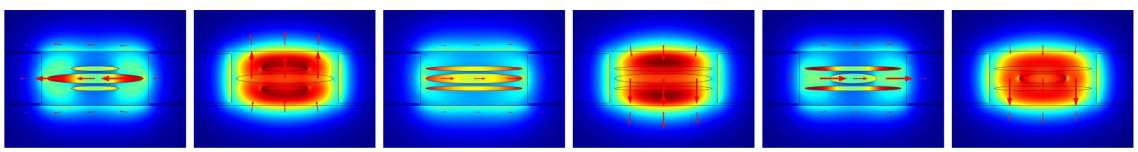

Fig. 2 Electric field distribution for **a** *x*-pol mode when $L > L1$, **b** *y*-pol mode when $L > L1$, **c** *x*-pol mode when $L = L1$, **d** *y*-pol mode when $L = L1$, **e** *x*-pol mode when $L < L1$, **f** *y*-pol mode when $L < L1$,

By inserting the real part of *x* and *y* polarization effective mode index value into Eq. 1, we have calculated the birefringence and plotted in the Fig. 4a at different major axes length variation by keeping the pitch among the ellipses as constant of its optimum value. It can be seen that the birefringence of the proposed PCF is increasing along with operating frequency increment. The maximum birefringence of 0.0921 is obtained when the length of the major axis of all three ellipses is equal and the equal length is 200 µm. For $L > L1$condition, length of center ellipse was kept 200 µm and the length of $L1$ decreased by 50% of L. Similarly, for $L < L1$, length of $L1$ was 200 µm and the center ellipse length decreased by 50% of $L1$. For higher major axis length of upper and lower ellipse than the center ellipse produces the lowest birefringence of 0.0732 at 1 THz operating frequency. Because, when the center ellipse length is less than the other two ellipses in the core region it produces more confinement loss in the fiber. For these reasons, the real part of effective mode indices difference between the x and y polarization modes is significantly lower than the equal major axis length.

Again, we kept the major axis and minor axis length constant during the pitch variation among the ellipse.

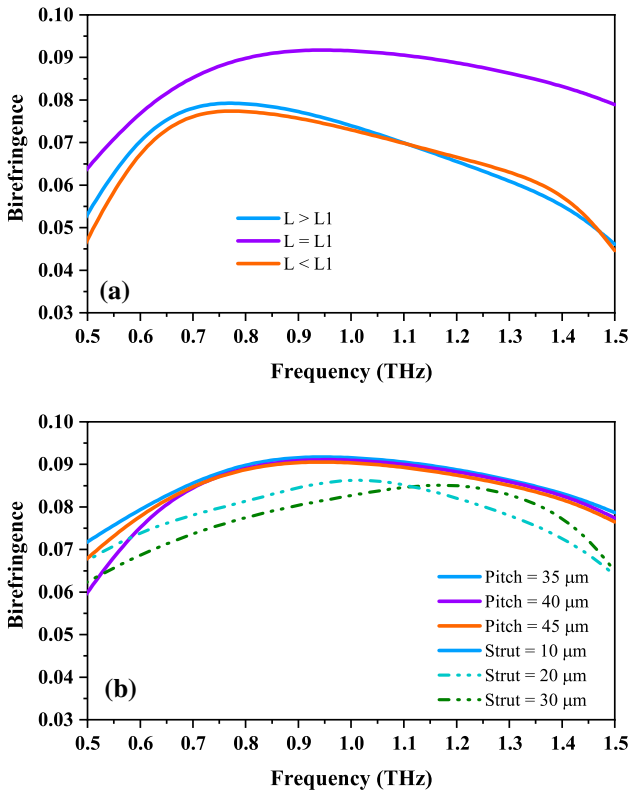

Fig. 4 Birefringence characteristics of the suggested PCF **a** with various length combination ($L > L1, L = L1, L < L1$), **b** with various pitch and strut combination ($pitch = 35\mu m$, $pitch = 40\mu m$, $pitch = 45\mu m$, $strut = 10\mu m$, $strut = 20\mu m$, $strut = 30\mu m$)

Figure 4b shows the birefringence characteristics at different pitch variations of ellipse and strut variations of rectangular air hole slots along with frequency. We varied the center to center distance of the ellipse by 5 µm started from 40 µm. When the pitch distance is increased by 5 µm from 40 µm, the birefringence of the proposed PCF is decreased. But, When the pitch distance is decreased by 5 µm from 40 µm, the birefringence of the proposed PCF is increased. This phenomenon leads the scenario that when the ellipses in the core region are closer it allows producing more light confinement through the core region. But, when the ellipses are so close to each other it will arise the fabrication complexity. Again, we varied the strut distance among the rectangular air hole slots from 10 to 30 µm where strut distance is denoted as q on the Fig. 1a. We found that for minimum strut distance of 10 µm the proposed PCF produced high birefringence. So, to make our proposed PCF as fabrication friendly, we have chosen the pitch distance among the adjacent ellipse as 35 µm and strut distance among the air hole slots as 10 µm.

Another important factor to consider for designing a PCF is effective material loss calculation. Using the following calculation, EML of the suggested PCF is estimated [20]

$$\text{EML}\ (\alpha_{eff}) = \sqrt{\frac{\epsilon_0}{\mu_0}}\left(\frac{\int_{mat} n_{mat}|E|^2\alpha_{mat}dA}{\frac{1}{2}|\int_{all}(E\times H.z)dA|}\right),\ \text{cm}^{-1} \tag{2}$$

where n_{mat} and α_{mat} represents the refractive index and bulk material absorption loss of Topas glass respectively. ϵ_0 is relative permittivity and μ_0 is the relative permeability in the free space. E and H represents the electric field and the magnetic field accordingly. Effective material loss is calculated per centimeter length of the proposed PCF and TM mode propagation is considered during calculation. Figure 5a shows the dependency of effective material loss on ellipse major axes length variation as a function of frequency. EML is less when the length of the center ellipse major axis is equal with rest ellipses' major axes lengthuntil 0.95 THz. As we described in the Eq. 2, EML is mostly depending on the electric field distribution on the PCF. When the operating frequency increase the, the electric field distribution reduce from the core region area and increase on the cladding region. The EML change due to pitch variation is showing in Fig. 5b. Effective material loss of $1.49 \times 10^{-4}\text{cm}^{-1}$has been achieved at 1 THz operating frequency when the pitch distance is 35 µm with equal major axis length of all core ellipses.

After observing the birefringence and effective material loss calculations, the optimal major axis length is found 200 µm and center to center distance among the ellipse is 35 µm. Using these optimal conditions, we have also investigated the confinement loss of the proposed PCF. Confinement loss defines the ability of light confinement

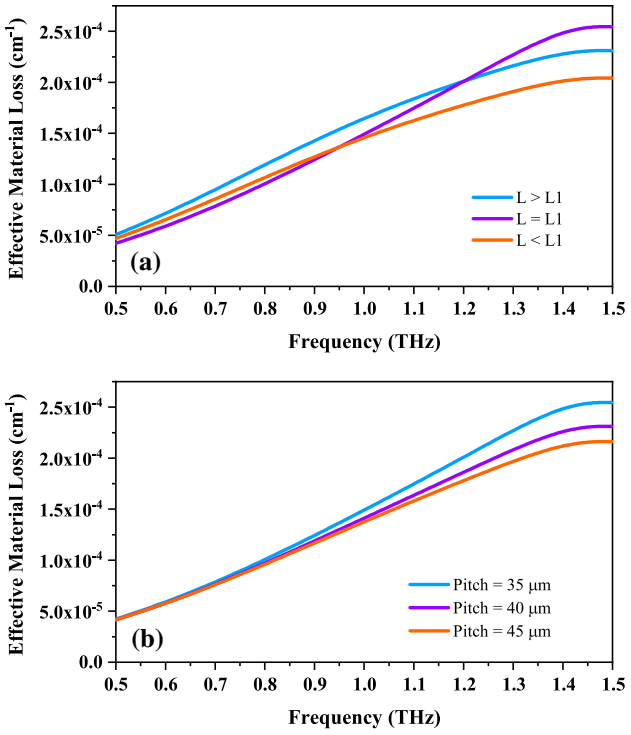

Fig. 5 Effective material loss characteristics of the suggested PCF **a** with various length combination ($L > L1, L = L1, L < L1$), **b** with various pitch combination (*pitch* = 35µm, *pitch* = 40µm, *pitch* = 45µm)

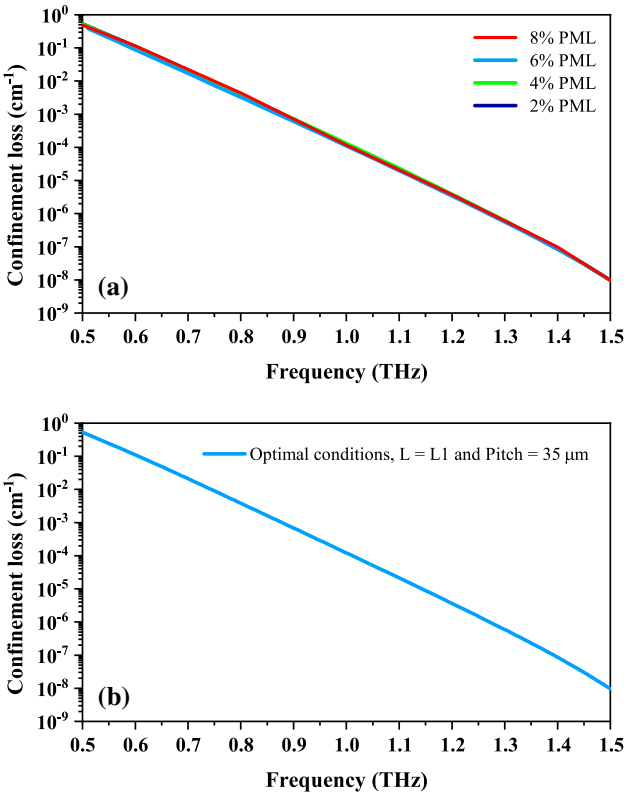

Fig. 6 **a** Effect of PML thickness on Confinement loss, **b** Confinement loss of the proposed PCF at optimal conditions

into a PCF core rather than the cladding region. The less confinement loss indicates better light confinement into the center part of the PCF. In PCF, light isolation within its central area increases significantly when air-holes or slots rise in the cladding. As per the theoretical explanation, the confinement loss should be zero if an infinite number of air holes used in PCF [21]. Nevertheless, within a PCF, the countable air holes are required for real-life applications and feasible to produce. The confinement loss of a PCF can be defined by the following equation [22]

$$\text{Confinement loss } (L) = \left(\frac{4\pi f}{c}\right)\text{Im}(n_{eff}), \text{cm}^{-1} \quad (3)$$

where f, c and $\text{Im}(n_{eff})$ represents operating frequency in THz, velocity of light and imaginary part of effective mode index respectively. At optimum conditions, we have investigated the effects of PML layer thickness variations on confinement loss in Fig. 6a. For numerical analysis of a PCF, researchers are chosen PML thickness from 2 to 10% of its total fiber diameter [13, 20, 23, 24]. The Fig. 6a shows that there is a less significant effect of PML thickness variation on confinement loss. We have varied the PML thickness from 2 to 8% of the total fiber diameter. If we increase the PML layer more than 10% then PML will overlap with cladding rectangular air slots. At optimum conditions and 1 THz operating frequency, 6% PML thickness of the total fiber diameter shows the best results for the proposed PCF. Confinement loss characteristics of the suggested PCF with 6% PML is presented in Fig. 6b along with frequency. At 1 THz operating frequency, we obtained confinement loss of the PCF is 1.36×10^{-4} cm^{-1} which is comparable with recently proposed PCF [13, 14, 25, 26].

In Fig. 7, black and blue line represents the dispersion and effective mode area (A_{eff}) of the proposed PCF respectively at optimal conditions. The dispersion of the

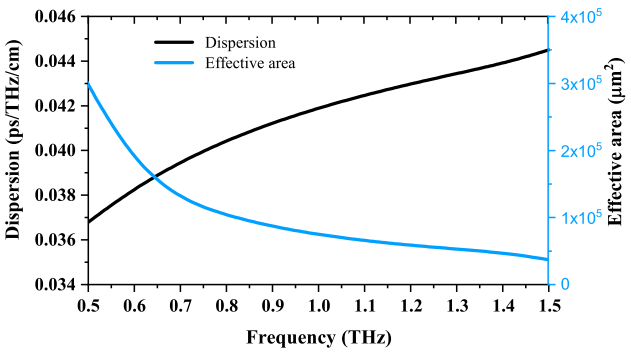

Fig. 7 Dispersion and Effective mode area of the proposed PCF at optimal conditions

Table 1 Detail comparisons of proposed PCF with recently reported PCF

Ref.	f (THz)	B	α_{eff} (cm^{-1})	L (cm^{-1})
[24]	1	0.011	0.015	–
[12]	3	0.030	0.06	2.30×10^{-5}
[26]	0.85	0.033	0.099	1.58×10^{-4}
[31]	1	0.045	0.08	–
[13]	1	0.048	0.085	4.39×10^{-4}
[14]	1.2	0.051	0.07	1.65×10^{-3}
[25]	1	0.075	0.07	1.84×10^{-3}
This study	1	0.0921	1.49×10^{-4}	1.36×10^{-4}

proposed PCF is calculated by Eq. 4 at which ω is the angular frequency, n_{eff} real part of effective refractive index and c is the speed of light in vacuum [27]. At 1 THz operating frequency, we found a very low dispersion of 0.041 ps/THz/cm for the proposed PCF which is comparable with recently reported research [27, 28].

$$d = \left(\frac{2}{c} \times \frac{dn_{eff}}{d\omega}\right) + \left(\frac{\omega}{c} \times \frac{d^2 n_{eff}}{d\omega^2}\right) \text{ps/THz/cm} \quad (4)$$

At lower THz frequency, the light confined into the PCF closely which tends the guiding waves to spread largely [23]. So, with increasing frequency the A_{eff} are decreasing that reflects on the Fig. 7. At 1 THz frequency with optimal conditions the obtained effective mode area for the proposed PCF is 7.33×10^4 μm^2. Effective mode area (A_{eff}) of the proposed PCF is calculated by the Eq. 5 at which E is the propagating medium's electrical field vector[20].

$$A_{eff} = \frac{(\int\int |E|^2 dxdy)^2}{\int\int |E|^4 dxdy}, \mu m^2 \quad (5)$$

The distinction of our suggested PCF with recently reported THz-based PCF is shown in Table 1. Our proposed PCF is well ahead of the reported PCF in terms of birefringence, effective material loss and confinement loss. The proposed PCF will be very effective for polarization maintaining devices and other applications as it exhibits a simple geometric structure than other reported PCF. There are several fabrication technology, but the extrusion and 3D printing fabrication technology are potentially able to fabricate any types of asymmetrical PCF structure[20, 29, 30] . By employing the existing PCF fabrication technologies, we hope the proposed PCF is feasible to fabricate.

4 Conclusion

In this study, a highly birefringent PCF has been designed that will be able to maintain the polarization during propagation by its high birefringence characteristics in THz frequency region. Moreover, the designed elliptical core based PCF has lower effective material loss and confinement loss compared to recently proposed PCF. To get the asymmetric conditions, rectangular shaped air holes in the cladding region has been considered along with elliptical air holes in the core region. Numerical analysis shows that high birefringence of 0.0921, effective material loss of 1.49×10^{-4} cm^{-1} and confinement loss of 1.36×10^{-4} cm^{-1} at 1 THz operating frequency along with effective mode area of 7.33×10^4 μm^2 has been achieved for the proposed PCF. Dependency of core major axis length, pitch among the core air holes, strut distance within the cladding has been considered to characterize birefringence of the proposed PCF. Moreover, geometrical parameters of the PCF has been fully optimized and used only three elliptical air holes in the core region in order to increase the manufacturing efficiency. We strongly believe that, the proposed PCF will contribute to the practical applications of polarization filter, sensing and terahertz communication systems and polarization preserving fibers.

Compliance with ethical standards

Conflict of interest The authors declare that they have no conflict of interest.

References

1. Russell PSJ (2006) Photonic-crystal fibers. J Lightwave Technol 24(12):4729–4749
2. Zhang L, Ren G-J, Yao J-Q (2013) A new photonic crystal fiber gas sensor based on evanescent wave in terahertz wave band: design and simulation. Optoelectron Lett 9(6):438–440
3. Ramachandran A, Babu PR, Senthilnathan K (2017) Sensitivity analysis of steering-wheel gas sensor against diverse core air hole sizes and core materials in terahertz wave band. In: Materials science and engineering conference series, 263:052036 (2017)
4. Sen S, Ahmed K (2019) Design of terahertz spectroscopy based optical sensor for chemical detection. SN Appl Sci 1(10):1215
5. Kanmani R, Ahmed K, Roy S, Ahmed F, Paul BK, Rajan MM (2019) The performance of hosting and core materials for slotted core q-pcf in terahertz spectrum. Optik 194:163084
6. Liu Q, Li S, Chen H, Li J, Fan Z (2015) High-sensitivity plasmonic temperature sensor based on photonic crystal fiber coated with nanoscale gold film. Applied Physics Express 8(4):046701
7. Hossain MB, Podder E, Bulbul AA-M, Mondal HS (2020) Bane chemicals detection through photonic crystal fiber in thz regime. Opt Fiber Technol 54:102102

8. Hossain MB, Podder E (2019) Design and investigation of pcf-based blood components sensor in terahertz regime. Appl Phys A 125(12):861
9. Zhang Y, Xue L, Qiao D, Guang Z (2019) Porous photonic-crystal fiber with near-zero ultra-flattened dispersion and high birefringence for polarization-maintaining terahertz transmission. Optik 163817 (2019)
10. Prabu K, Malavika R (2019) Highly birefringent photonic crystal fiber with hybrid cladding. Opt Fiber Technol 47:21–26
11. Saha R, Hossain MM, Rahaman ME, Mondal HS (2019) Design and analysis of high birefringence and nonlinearity with small confinement loss photonic crystal fiber. Front Optoelectron 12(2):165–173
12. Wu Z, Shi Z, Xia H, Zhou X, Deng Q, Huang J, Jiang X, Wu W (2016) Design of highly birefringent and low-loss oligoporous-core thz photonic crystal fiber with single circular air-hole unit. IEEE Photonics J 8(6):1–11
13. Hasan MR, Anower MS, Islam MA, Razzak S (2016) Polarization-maintaining low-loss porous-core spiral photonic crystal fiber for terahertz wave guidance. Appl Opt 55(15):4145–4152
14. Habib MA, Anower MS (2019) Design and numerical analysis of highly birefringent single mode fiber in thz regime. Opt Fiber Technol 47:197–203
15. Markos C, Stefani A, Nielsen K, Rasmussen HK, Yuan W, Bang O (2013) High-tg topas microstructured polymer optical fiber for fiber bragg grating strain sensing at 110 degrees. Opt Express 21:4758–4765
16. Paul BK, Ahmed K (2019) Highly birefringent topas based single mode photonic crystal fiber with ultra-low material loss for terahertz applications. Opt Fiber Technol 53:102031
17. Rahaman ME, Saha R, Ahsan MS, Sohn I-B (2018) Design and performance analysis of a d–shaped pcf and surface plasmon resonance based glucose sensor. In: 2018 4th International conference on electrical engineering and information & communication technology (iCEEiCT). IEEE, pp 325–329
18. Islam MS, Sultana J, Atai J, Abbott D, Rana S, Islam MR (2017) Ultra low-loss hybrid core porous fiber for broadband applications. Appl Opt 56(4):1232–1237
19. Sidhik S, Ittiarah JV, Pal M, Gangopadhyay TK (2019) All-circular hole microstructured fiber with ultra-high birefringence and reduced confinement loss. Measurement 147:106895
20. Islam MR, Kabir MF, Talha KMA, Islam MS (2019) A novel hollow core terahertz refractometric sensor. Sens Bio-Sens Res 25:100295
21. Matsui T, Zhou J, Nakajima K, Sankawa I (2005) Dispersion-flattened photonic crystal fiber with large effective area and low confinement loss. J Lightwave Technol 23(12):4178–4183
22. Saitoh K, Koshiba M (2003) Leakage loss and group velocity dispersion in air-core photonic bandgap fibers. Opt Express 11(23):3100–3109
23. Sen S, Islam MS, Paul BK, Islam MI, Chowdhury S, Ahmed K, Hasan MR, Uddin MS, Asaduzzaman S (2019) Ultra-low loss with single mode polymer-based photonic crystal fiber for thz waveguide. J Opt Commun 40(4):411–417
24. Ahmed K, Chowdhury S, Paul BK, Islam MS, Sen S, Islam MI, Asaduzzaman S (2017) Ultrahigh birefringence, ultralow material loss porous core single-mode fiber for terahertz wave guidance. Appl Opt 56(12):3477–3483
25. Islam R, Habib MS, Hasanuzzaman G, Ahmad R, Rana S, Kaijage SF (2015) Extremely high-birefringent asymmetric slotted-core photonic crystal fiber in thz regime. IEEE Photonics Technol Lett 27(21):2222–2225
26. Hasanuzzaman G, Rana S, Habib MS (2016) A novel low loss, highly birefringent photonic crystal fiber in thz regime. IEEE Photonics Technol Lett 28(8):899–902
27. Sultana J, Islam MS, Faisal M, Islam MR, Ng BW-H, Ebendorff-Heidepriem H, Abbott D (2018) Highly birefringent elliptical core photonic crystal fiber for terahertz application. Opt Commun 407:92–96
28. Islam MS, Sultana J, Atai J, Islam MR, Abbott D (2017) Design and characterization of a low-loss, dispersion-flattened photonic crystal fiber for terahertz wave propagation. Optik 145:398–406
29. Atakaramians S, Afshar S, Ebendorff-Heidepriem H, Nagel M, Fischer BM, Abbott D, Monro TM (2009) Thz porous fibers: design, fabrication and experimental characterization. Opt Express 17(16):14053–14062
30. Ebendorff-Heidepriem H, Schuppich J, Dowler A, Lima-Marques L, Monro TM (2014) 3d-printed extrusion dies: a versatile approach to optical material processing. Opt Mater Express 4(8):1494–1504
31. Islam R, Habib MS, Hasanuzzaman G, Rana S, Sadath MA (2016) Novel porous fiber based on dual-asymmetry for low-loss polarization maintaining thz wave guidance. Opt Lett 41(3):440–443